Integro-differential form of the first-order dual phase lag heat transfer equation and its numerical solution using the Control Volume Method

M. CIESIELSKI[1)], B. MOCHNACKI[2)], E. MAJCHRZAK[3)]

[1)] *Czestochowa University of Technology, Dabrowskiego 73, 42-201 Czestochowa, Poland, e-mail:mariusz.ciesielski@icis.pcz.pl (corresponding author)*

[2)] *University of Occupational Safety Management, Bankowa 8, 40-007 Katowice, Poland, e-mail:bmochnacki@wszop.edu.pl*

[3)] *Silesian University of Technology, Konarskiego 18A, 44-100 Gliwice, Poland, e-mail:ewa.majchrzak@polsl.pl*

THE START POINT OF THE DUAL PHASE LAG EQUATION (DPLE) formulation is the generalized Fourier law in which two positive constants (the relaxation and thermalization times) appear. This type of equation can be used (among others) to describe the heat conduction processes proceeding in micro-scale. Depending on the number of components in the development of the generalized Fourier law into a power series, one can obtain both the first-order DPLE and the second-order one. In this paper the first-order dual phase lag equation is considered. The primary objective of this research is the transformation of DPLE differential form to the integro-differential one supplemented by the appropriate boundary-initial conditions. The obtained form of the differential equation is much simpler and more convenient at the stage of numerical computations – the numerical algorithm based on the three-time-level scheme reduces to the two-time-level one. To find the numerical solution, the Control Volume Method is used (the heating of thin metal film subjected to a laser beam is considered). The choice of the numerical method was not accidental. The method has a simple physical interpretation ensuring the preservation of the local and global energy balances. To our knowledge, it has not been used so far in this type of tasks. In the final part of the paper the examples of numerical simulations are presented and the conclusions are formulated.

Key words: micro-scale heat transfer, dual phase lag model, integro-differential equation, Control Volume Method.

Notation

c	volumetric specific heat [J/(m^3 K)],
f	level of time,
I_0	laser intensity [J/m^2],
L	domain depth for 1D task [m],
$\mathbf{n}$	outward unit normal vector,
$\mathbf{q}(\mathbf{x}, t)$	heat flux vector [W/m^2],

$\mathbf{q}_0$	initial heat flux [W/m^2],
q_b	boundary heat flux [W/m^2],
Q	capacity of internal heat sources [W/m^3],
r_d	characteristic radius of Gaussian laser beam [m],
R, Z	radius and height of axially-symmetrical domain for 2D task [m],
R_f	reflectivity of irradiated surface,
T	temperature [K],
T_0, T_1	initial conditions [K],
T_{out}	ambient temperature [K],
t	time [s],
t_p	characteristic time of laser pulse [s],
$\mathbf{x}, x, r, z$	geometrical co-ordinates [m],
ΔV_i	volume of Ω_i [m^3].

Greek letters

α	heat transfer coefficient [W/(m^{2}K)],
δ	optical penetration depth [m],
Γ	boundary of domain,
λ	thermal conductivity [W/(m K)],
Φ	shape functions of CVM mesh,
τ_q	relaxation time [s],
τ_T	thermalization time [s],
Ω	domain,
Ω_i	i-th control volume.

1. Introduction

IN THIS PAPER, THE FIRST ORDER DUAL-PHASE LAG EQUATION [1–4] is applied
for numerical modeling of thermal processes in the domain of thin metal film sub-
jected to a laser pulse [5, 6]. Thus, the problem related to the microscale heat
transfer is discussed. Heat transfer through the metal microdomains affected by
the laser beam is of the vital importance in microtechnology applications and
it is a reason that the problem related to the fast heating of solids has become
a very active research area. The characteristics of such a process are the ex-
tremely short duration, the extreme temperature gradients and the very small
dimensions of the domain considered The very high heating rates typical for the
micro-scale heat transfer cause that the finite value of thermal wave velocity
should be somehow taken into account. The effect of local and temporary lag
of heat flux in relation to the temperature gradient was taken into account by
CATTANEO [7]. In particular, the modification of Fourier's law has been pro-
posed and finally the hyperbolic energy equation called the Cattaneo–Vernotte
equation has been obtained. The similar approach leads to the dual-phase lag
model but the generalization of the Fourier law results from the introduction of
two lag times (e.g. [8]), namely

$$(1.1) \qquad\qquad \mathbf{q}(x, t + \tau_q) = -\lambda \nabla T(x, t + \tau_T)$$

where $\mathbf{q}$ is a heat flux vector, ∇T is a temperature gradient, λ is a thermal conductivity, $\mathbf{x}$, t denote the geometrical co-ordinates and time. The positive constants τ_q, τ_T correspond to the relaxation time and thermalization time, respectively. The relaxation time τ_q takes into account the small-scale response in time, while the thermalization time τ_T takes into account the small-scale response in space [9, 10]. The formula (1.1) is developed into the Taylor series and depending on the order of development (after using the well-known energy balance equation) the first- or the second-order DPLE is obtained [11, 12]. The mixed variants are also considered, for example the left hand side of equation is the same as in the case of the second-order model, while the right hand side corresponds to the first-order model [13, 14]. In the papers [15–17] the basic form of DPLE is modified using the substitution techniques (the paper [15] concerns the first-order DPLE). It should be pointed out, that the solutions of higher-order DPLE can be incorrect and this fact results from the limitations concerning the values of lag times. These problems are discussed in [18–20]. As mentioned previously, this work involves the transformation of the first order DPLE.

In literature one can find the analytical or semi-analytical solutions of the first-order DPLE concerning, as a rule, the 1D problems. In this paper the results of numerical computations are compared with the analytical solution presented by CIESIELSKI in [21]. The other analytical solution concerning the similar task using the Green function method and finite integral transform technique can be found in [22]. In turn, in the paper [23] the multi-layered cylindrical and spherical domains are considered and the solution is obtained by means of the Laplace transform method. In recent years the dual-phase lag model has been applied for the analysis of thermal processes occurring in the domain of biological tissue. The analytical solutions of DPL bio-heat transfer equation are presented in [24, 25]. The analytical solution of the three-dimensional DPLE using the Adomian decomposition method (ADM) can be found in [26]. The exact solution of the lagging model for the semi-infinite medium is discussed in [27].

In the vast majority of the works associated with the practical aspects of DPLE solutions the numerical methods are used, mainly the different variants of the finite difference method. Restricting only to the first-order equations, one can (as an example), mention works [5, 11, 12, 14, 15, 28, 29]. The others numerical methods are also applied, of course. Here one can replace the control volume method (e.g. [30–32]), the boundary element method (e.g. [33]) or the finite element method (e.g. [34]).

The work consists of six sections. In Section 2 the governing equations creating the classical dual-phase lag model and its integro-differential modification are discussed. A mathematical form of the appropriate boundary-initial conditions is also formulated. Section 3 is devoted to the presentation of the authorial numer-

ical algorithm based on the control volume method. In Section 4 the 1D and 2D axially-symmetrical problems concerning the thin metal film heating are considered. The laser action is taken into account by the introduction of the artificial internal heat source $Q(\mathbf{x}, t)$ – this approach is very often used. The second part of this Section is devoted to details concerning the numerical solution of the task formulated. Also, in this Section the examples of computations are presented. In particular, the heating/cooling process in the domain of thin metal film (gold, chromium, nickel) subjected to a laser pulse is considered. Next, the verification and analysis of numerical solutions are studied. The solutions obtained are compared, among others, with the analytical ones discussed in [21]. The last section contains the conclusions and final remarks resulting from conducted research.

2. Governing equations

The domain $\Omega \subset \mathbb{R}^d$, $d = 1, 2, 3$, bounded by the boundary Γ is considered.

As mentioned in the introduction the starting point for the considerations is the assumption that the heat conduction in solids results from the generalized Fourier law (1.1). The dependence containing the time delays makes difficult to find the general solution for the temperature. The usual approach to study the effects of the dual phase lag model results from the Taylor series expansion. The first-order approximations for $\mathbf{q}$ as well as for ∇T occurred in formula (1.1) lead to the equation

$$(2.1) \qquad \mathbf{q}(\mathbf{x}, t) + \tau_q \frac{\partial \mathbf{q}(\mathbf{x}, t)}{\partial t} = -\lambda \left[\nabla T(\mathbf{x}, t) + \tau_T \frac{\partial \nabla T(\mathbf{x}, t)}{\partial t} \right]$$

which is often called the first-order dual-phase-lagging constitutive equation. The above formula can be treated as a differential equation and should be supplemented by the initial conditions for $\mathbf{q}$ and ∇T.

The second important equation is the general energy balance equation which can be written as

$$(2.2) \qquad c \frac{\partial T(\mathbf{x}, t)}{\partial t} = -\nabla \cdot \mathbf{q}(\mathbf{x}, t) + Q(\mathbf{x}, t)$$

where c is a volumetric specific heat, the function $Q(\mathbf{x}, t)$ is a capacity of internal heat sources (e.g. related to the laser heating).

The 'natural' initial condition for Eq. (2.2) is given in the form

$$(2.3) \qquad T(\mathbf{x}, 0) = T_0(\mathbf{x}).$$

Also, the other forms of initial conditions for Eq. (2.2) can be used. The following initial condition results directly from Eq. (2.2), for $t = 0$,

$$(2.4) \qquad \left. \frac{\partial T(\mathbf{x}, t)}{\partial t} \right|_{t=0} = \frac{-\nabla \cdot \mathbf{q}(\mathbf{x}, 0) + Q(\mathbf{x}, 0)}{c} = T_1(\mathbf{x}).$$

If $Q(\mathbf{x}, 0) = 0$ and $\nabla \cdot \mathbf{q}(\mathbf{x}, 0) = 0$, then the initial condition is $T_1(\mathbf{x}) = 0$. But, if the source function Q is described by, for example, the Gaussian-type function then for $t = 0$: $Q(\mathbf{x}, t)|_{t=0} \neq 0$ and this initial condition should be taken into account in order to ensure the energy balance of the system.

2.1. Differential form of DPLE

Applying the divergence operator to both sides of Eq. (2.1) and introducing the divergence term $\nabla \cdot \mathbf{q}(\mathbf{x}, t)$ from Eq. (2.2) into the obtained formula, the following differential equation determining the transient temperature field in the domain considered is formulated

$$(2.5) \qquad c\left(\frac{\partial T(\mathbf{x}, t)}{\partial t} + \tau_q \frac{\partial^2 T(\mathbf{x}, t)}{\partial t^2}\right)$$
$$= \lambda\left(\nabla^2 T(\mathbf{x}, t) + \tau_T \frac{\partial \nabla^2 T(\mathbf{x}, t)}{\partial t}\right) + Q(\mathbf{x}, t) + \tau_q \frac{\partial Q(\mathbf{x}, t)}{\partial t}$$

which should be supplemented by the initial conditions (2.3)–(2.4) and the appropriate boundary conditions.

2.2. Integro-differential form of DPLE

The combination of the constitutive equation for heat transfer (2.1) and the energy conservation equation (2.2) can be also realized in another way. One can notice that Eq. (2.1) can be treated as a differential equation. The general solution of this equation with respect to function $\mathbf{q}(\mathbf{x}, t)$ (obtained on the basis of the solution discussed in [35]) is the following

$$(2.6) \qquad \mathbf{q}(\mathbf{x}, t)$$
$$= \exp\left(-\frac{t}{\tau_q}\right)\left[C(\mathbf{x}) - \frac{\lambda}{\tau_q}\int \exp\left(\frac{t}{\tau_q}\right)\left(\nabla T(\mathbf{x}, t) + \tau_T \frac{\partial \nabla T(\mathbf{x}, t)}{\partial t}\right) \mathrm{d}t\right]$$

where C is an arbitrary integration "constant" depending on the variable $\mathbf{x}$ and it should be determined in the case to find the particular solution satisfying any initial condition In this work, the following initial condition at $t = 0$ is taken into account

$$(2.7) \qquad\qquad\qquad \mathbf{q}(\mathbf{x}, 0) = \mathbf{q}_0(\mathbf{x}).$$

Alternatively, the first order differential Eq.(2.1) with the initial condition (2.7) can be also solved with respect to function $\mathbf{q}(\mathbf{x}, t)$ by the Laplace transform method [35]. Taking the Laplace transformation on both sides of Eq. (2.1) one obtains

$$\mathcal{L}\{\mathbf{q}(\mathbf{x},t)\}(s)+\tau_q\mathcal{L}\left\{\frac{\partial\mathbf{q}(\mathbf{x},t)}{\partial t}\right\}(s)=-\lambda\mathcal{L}\left\{\nabla T(\mathbf{x},t)+\tau_T\frac{\partial\nabla T(\mathbf{x},t)}{\partial t}\right\}(s),$$

(2.8) $\quad\tilde{\mathbf{q}}(\mathbf{x},s)+\tau_q(s\,\tilde{\mathbf{q}}(\mathbf{x},s)-\mathbf{q}_0(\mathbf{x}))=-\lambda\tilde{\tilde{T}}(\mathbf{x},s),$

$$\tilde{\tilde{T}}(\mathbf{x},s)=\mathcal{L}\left\{\nabla T(\mathbf{x},t)+\tau_T\frac{\partial\nabla T(\mathbf{x},t)}{\partial t}\right\}(s).$$

Solving for $\tilde{\mathbf{q}}(\mathbf{x},s)$ we have

(2.9) $$\tilde{\mathbf{q}}(\mathbf{x},s)=-\frac{\lambda\tilde{\tilde{T}}(\mathbf{x},s)}{\tau_q s+1}+\frac{\tau_q\,\mathbf{q}_0(\mathbf{x})}{\tau_q s+1}.$$

Next, using the inverse Laplace transform we get the solution in time domain

(2.10) $\quad\mathbf{q}(\mathbf{x},t)=\mathcal{L}^{-1}\{\tilde{\mathbf{q}}(\mathbf{x},s)\}(t)$

$$=-\frac{\lambda}{\tau_q}\mathcal{L}^{-1}\left\{\frac{\tilde{\tilde{T}}(\mathbf{x},s)}{s+\tau_q^{-1}}\right\}(t)+\mathbf{q}_0(\mathbf{x})\mathcal{L}^{-1}\left\{\frac{1}{s+\tau_q^{-1}}\right\}(t)$$

$$=-\frac{\lambda}{\tau_q}\exp\left(-\frac{t}{\tau_q}\right)*\left(\nabla T(\mathbf{x},t)+\tau_T\frac{\partial\nabla T(\mathbf{x},t)}{\partial t}\right)+\exp\left(-\frac{t}{\tau_q}\right)\mathbf{q}_0(\mathbf{x}).$$

By applying the convolution integral and sum rule of integration, the above particular solution can be expressed in the form

(2.11) $\quad\mathbf{q}(\mathbf{x},t)$

$$=-\frac{\lambda}{\tau_q}\int_0^t\exp\left(-\frac{t-u}{\tau_q}\right)\left(\nabla T(\mathbf{x},u)+\tau_T\frac{\partial\nabla T(\mathbf{x},u)}{\partial u}\right)du+\exp\left(-\frac{t}{\tau_q}\right)\mathbf{q}_0(\mathbf{x})$$

$$=-\lambda\left(\frac{1}{\tau_q}\int_0^t\exp\left(-\frac{t-u}{\tau_q}\right)\nabla T(\mathbf{x},u)\,du+\frac{\tau_T}{\tau_q}\int_0^t\exp\left(-\frac{t-u}{\tau_q}\right)\frac{\partial\nabla T(\mathbf{x},u)}{\partial u}\,du\right)$$

$$+\exp\left(-\frac{t}{\tau_q}\right)\mathbf{q}_0(\mathbf{x}).$$

Next, by using the integration by parts formula to the second integral in Eq. (2.11):

(2.12) $$\int_0^t\exp\left(-\frac{t-u}{\tau_q}\right)\frac{\partial\nabla T(\mathbf{x},u)}{\partial u}\,du$$

$$=\exp\left(-\frac{t-u}{\tau_q}\right)\nabla T(\mathbf{x},u)\big|_0^t-\int_0^t\frac{1}{\tau_q}\exp\left(-\frac{t-u}{\tau_q}\right)\nabla T(\mathbf{x},u)\,du$$

$$=\nabla T(\mathbf{x},t)-\exp\left(-\frac{t}{\tau_q}\right)\nabla T(\mathbf{x},0)-\frac{1}{\tau_q}\int_0^t\exp\left(-\frac{t-u}{\tau_q}\right)\nabla T(\mathbf{x},u)\,du$$

and subsequent transformations of this equation lead to the form

$$(2.13) \quad \mathbf{q}(\mathbf{x}, t) = -\lambda \left(\frac{1}{\tau_q} \int_0^t \exp\left(-\frac{t-u}{\tau_q}\right) \nabla T(\mathbf{x}, u) \, du + \frac{\tau_T}{\tau_q} \nabla T(\mathbf{x}, t) \right.$$

$$-\frac{\tau_T}{\tau_q} \exp\left(-\frac{t}{\tau_q}\right) \nabla T(\mathbf{x}, 0) - \frac{\tau_T}{\tau_q^2} \int_0^t \exp\left(-\frac{t-u}{\tau_q}\right) \nabla T(\mathbf{x}, u) \, du \right)$$

$$+ \exp\left(-\frac{t}{\tau_q}\right) \mathbf{q}_0(\mathbf{x})$$

$$= -\lambda \left(\frac{\tau_T}{\tau_q} \nabla T(\mathbf{x}, t) - \frac{\tau_T}{\tau_q} \exp\left(-\frac{t}{\tau_q}\right) \nabla T(\mathbf{x}, 0) \right.$$

$$+ \frac{\tau_q - \tau_T}{\tau_q^2} \int_0^t \exp\left(-\frac{t-u}{\tau_q}\right) \nabla T(\mathbf{x}, u) \, du \right) + \exp\left(-\frac{t}{\tau_q}\right) \mathbf{q}_0(\mathbf{x})$$

or

$$(2.14) \qquad \mathbf{q}(\mathbf{x}, t) = -\lambda \frac{\tau_T}{\tau_q} (\nabla T(\mathbf{x}, t) - s_q(t) \nabla T(\mathbf{x}, 0))$$

$$- \lambda \int_0^t K_q(t - u) \nabla T(\mathbf{x}, u) \, du + s_q(t) \mathbf{q}_0(\mathbf{x})$$

where

$$(2.15) \qquad K_q(v) = \frac{\tau_q - \tau_T}{\tau_q^2} \exp\left(\frac{-v}{\tau_q}\right),$$

$$(2.16) \qquad s_q(t) = \exp\left(-\frac{t}{\tau_q}\right).$$

Equation (2.14) shows that the heat flux at the time t depends on the history of the temperature gradient in the whole time interval $[0, t]$. This proves that the heat flux has a thermal memory.

Introducing formula (2.14) into Eq. (2.2) one has

$$(2.17) \qquad c\frac{\partial T(\mathbf{x}, t)}{\partial t} = \lambda \frac{\tau_T}{\tau_q} (\nabla^2 T(\mathbf{x}, t) - s_q(t) \nabla^2 T(\mathbf{x}, 0))$$

$$+ \lambda \int_0^t K_q(t - u) \nabla^2 T(\mathbf{x}, u) \, du - s_q(t)(\nabla \cdot \mathbf{q}_0(\mathbf{x})) + Q(\mathbf{x}, t).$$

From the formula (2.3) follows that $\nabla^2 T(\mathbf{x}, 0) = \nabla^2 T_0(\mathbf{x})$ and it can be directly introduced into Eq. (2.17). In turn, from Eq. (2.4) one has

$$\nabla \cdot \mathbf{q}_0(\mathbf{x}) = -cT_1(\mathbf{x}) + Q(\mathbf{x}, 0)$$

and this formula can be also putted into Eq. (2.17). Thus, the final integro-differential form of the DPLE is the following

$$(2.18) \qquad c\frac{\partial T(\mathbf{x}, t)}{\partial t} = \lambda\frac{\tau_T}{\tau_q}(\nabla^2 T(\mathbf{x}, t) - s_q(t)\nabla^2 T_0(\mathbf{x}))$$

$$+ \lambda\int_0^t K_q(t - u)\nabla^2 T(\mathbf{x}, u)\, du + s_q(t)(cT_1(\mathbf{x}) - Q(\mathbf{x}, 0)) + Q(\mathbf{x}, t)$$

while the initial condition is given by Eq. (2.3). A similar (in the mathematical sense) equation can be found in the work of Joseph and Preziosi [36], while the very general considerations about the integro-differential approach in [1].

2.3. Boundary conditions for the integro-differential equation

The Dirichlet boundary condition assumed on the part Γ of $\partial\Omega$ has a form

$$(2.19) \qquad \mathbf{x} \in \Gamma: \quad T(\mathbf{x}, t) = T_b(\mathbf{x}, t).$$

In the case of the Neumann boundary condition assumed on the part Γ of $\partial\Omega$, this means

$$(2.20) \qquad \mathbf{x} \in \Gamma: \quad \mathbf{n} \cdot \mathbf{q}(\mathbf{x}, t) = q_b(\mathbf{x}, t).$$

This condition should be converted into the form depending on the temperature gradient. Here $\mathbf{n}$ is an outward unit normal vector. Putting formula (2.14) into (2.20) one has

$$(2.21) \qquad \mathbf{x} \in \Gamma: \quad -\lambda\frac{\tau_T}{\tau_q}(\mathbf{n} \cdot \nabla T(\mathbf{x}, t) - s_q(t)(\mathbf{n} \cdot \nabla T(\mathbf{x}, 0)))$$

$$- \lambda\int_0^t K_q(t - u)(\mathbf{n} \cdot \nabla T(\mathbf{x}, u))\, du + s_q(t)(\mathbf{n} \cdot \mathbf{q}_0(\mathbf{x})) = q_b(\mathbf{x}, t).$$

Assuming for $\mathbf{x} \in \Gamma$ that $\mathbf{n} \cdot \mathbf{q}_0(\mathbf{x}) = q_b(\mathbf{x}, 0)$ and $\mathbf{n} \cdot \nabla T(\mathbf{x}, 0) = \mathbf{n} \cdot \nabla T_0(\mathbf{x})$

$$(2.22) \qquad \mathbf{x} \in \Gamma: \quad \frac{\tau_T}{\tau_q}(\mathbf{n} \cdot \nabla T(\mathbf{x}, t)) + \int_0^t K_q(t - u)(\mathbf{n} \cdot \nabla T(\mathbf{x}, u))\, du$$

$$= \frac{\tau_T}{\tau_q}(s_q(t)(\mathbf{n} \cdot \nabla T_0(\mathbf{x}))) - \frac{1}{\lambda}(q_b(\mathbf{x}, t) - s_q(t)q_b(\mathbf{x}, 0))$$

then the analytical solution of the above integral equation is of the form

$$(2.23) \qquad \mathbf{x} \in \Gamma: \quad -\lambda(\mathbf{n} \cdot \nabla T(\mathbf{x}, t)) = \frac{\tau_q}{\tau_T}(q_b(\mathbf{x}, t) - s_T(t)q_b(\mathbf{x}, 0))$$

$$+ \int_0^t K_T(t - u)q_b(\mathbf{x}, u)\, du - \lambda(s_T(t)(\mathbf{n} \cdot \nabla T_0(\mathbf{x})))$$

where

$$(2.24) \qquad K_T(v) = \frac{\tau_T - \tau_q}{\tau_T^2} \exp\left(-\frac{v}{\tau_T}\right),$$

$$(2.25) \qquad s_T(t) = \exp\left(-\frac{t}{\tau_T}\right).$$

The Robin boundary condition given on Γ (which was not used in this work), this means

$$(2.26) \qquad \mathbf{x} \in \Gamma: \quad \mathbf{n} \cdot \mathbf{q}(\mathbf{x}, t) = \alpha[T(\mathbf{x}, t) - T_{\text{out}}(\mathbf{x}, t)],$$

can be easy formulated by substitution $q_b(\mathbf{x}, t) = \alpha[T(\mathbf{x}, t) - T_{\text{out}}(\mathbf{x}, t)]$ into Eqs. (2.21) and (2.23).

It should be pointed out that for $q_b(\mathbf{x}, t)|_{\mathbf{x} \in \Gamma} = \bar{q}_b(\mathbf{x})|_{\mathbf{x} \in \Gamma}$ (which is a common case) the condition (2.23) reduces to the form

$$(2.27) \qquad \mathbf{x} \in \Gamma: \quad -\lambda(\mathbf{n} \cdot \nabla T(\mathbf{x}, t))$$

$$= \left(\frac{\tau_q}{\tau_T}(1 - s_T(t)) + \int_0^t K_T(t - u)\, du\right)\bar{q}_b(\mathbf{x}) - \lambda(s_T(t)(\mathbf{n} \cdot \nabla T_0(\mathbf{x})))$$

or after further transformations

$$(2.28) \qquad \mathbf{x} \in \Gamma: \quad -\lambda(\mathbf{n} \cdot \nabla T(\mathbf{x}, t)) = (1 - s_T(t))\bar{q}_b(\mathbf{x}) - \lambda(s_T(t)(\mathbf{n} \cdot \nabla T_0(\mathbf{x}))).$$

In the case of the adiabatic boundary condition (no flux b.c.) $q_b(\mathbf{x}, t)|_{\mathbf{x} \in \Gamma} = \bar{q}_b(\mathbf{x})|_{\mathbf{x} \in \Gamma} = 0$ the first term of the right hand side of Eq. (2.28) vanishes.

Now, the simplifications for particular cases of the initial conditions are discussed:

1. $\mathbf{q}_0(\mathbf{x}) = 0$. Then in Eq. (2.4) $\nabla \cdot \mathbf{q}(\mathbf{x}, 0) = 0$ and $T_1(\mathbf{x}) = Q(\mathbf{x}, 0)/c$. So, Eq. (2.18) simplifies to the form

$$(2.29) \qquad c\frac{\partial T(\mathbf{x}, t)}{\partial t}$$

$$= \lambda\frac{\tau_T}{\tau_q}(\nabla^2 T(\mathbf{x}, t) - s_q(t)\nabla^2 T_0(\mathbf{x})) + \lambda\int_0^t K_q(t - u)\nabla^2 T(\mathbf{x}, u)\, du + Q(\mathbf{x}, t).$$

2. $T_0(\mathbf{x}) = T_{\text{init}} = $ const. It follows from here $\nabla^2 T_0(\mathbf{x}) = 0$ and $\mathbf{n} \cdot \nabla T_0(\mathbf{x}) = 0$. The particular terms in equations (2.18), (2.29) as well as in the boundary conditions (2.23), (2.28) disappear. The mathematical model of such a process is significantly simpler.

3. Solution of equation using the control volume method

The control volume method (CVM) [30, 31, 32, 37] can be used, among others, to numerical solution of the heat diffusion equations. At first, the equation containing the divergence operators is integrated over the control volumes (so-called cells). Next, applying the Gauss theorem, the volume integral over the divergence is converted into a surface integral across the boundaries. These surface integrals can be calculated using suitable numerical methods for approximation of the sum of the fluxes across the boundary of the cells. The next stage of this method is a numerical approximation of time derivatives and time dependent integrals. The obtained system of algebraic equations allows one to find a set of unknowns (here the temporary temperature values at the nodes situated inside the control volumes).

Integration of Eq. (2.18) over the control volume Ω_i leads to

$$(3.1) \qquad c \int_{\Omega_i} \frac{\partial T(\mathbf{x}, t)}{\partial t}\, d\Omega = \lambda \frac{\tau_T}{\tau_q} \left(\int_{\Omega_i} \nabla^2 T(\mathbf{x}, t)\, d\Omega - s_q(t) \int_{\Omega_i} \nabla^2 T_0(\mathbf{x})\, d\Omega \right)$$

$$+ \lambda \int_0^t K_q(t-u) \int_{\Omega_i} \nabla^2 T(\mathbf{x}, u) d\Omega\, du + s_q(t) \left(c \int_{\Omega_i} T_1(\mathbf{x})\, d\Omega - \int_{\Omega_i} Q(\mathbf{x}, 0)\, d\Omega \right)$$

$$+ \int_{\Omega_i} Q(\mathbf{x}, t)\, d\Omega.$$

Let us introduce the functions $T_i(t)$ and $Q_i(t)$ which represent the average values of temperature and heat source in Ω_i, while ΔV_i, $i = 1, \ldots, N$ is the volume of Ω_i

$$(3.2) \qquad T_i(t) = \frac{1}{\Delta V_i} \int_{\Omega_i} T(\mathbf{x}, t)\, d\Omega \quad \text{and} \quad Q_i(t) = \frac{1}{\Delta V_i} \int_{\Omega_i} Q(\mathbf{x}, t)\, d\Omega.$$

Additionally

$$(3.3) \qquad \frac{dT_i(t)}{dt} = \frac{1}{\Delta V_i} \int_{\Omega_i} \frac{\partial T(\mathbf{x}, t)}{\partial t}\, d\Omega$$

and (see Eq. (2.4))

(3.4)
$$\bar{T}_{1i} = \frac{1}{\Delta V_i} \int\limits_{\Omega_i} T_1(\mathbf{x}) \, d\Omega.$$

Next, the function $\theta_i(t)$ in the form

(3.5)
$$\theta_i(t) = \frac{\lambda}{\Delta V_i} \int\limits_{\Omega_i} \nabla^2 T(\mathbf{x}, t) \, d\Omega = \frac{\lambda}{\Delta V_i} \int\limits_{A_i} \mathbf{n} \cdot \nabla T(\mathbf{x}, t) \, dA$$

$$= \frac{\lambda}{\Delta V_i} \sum_j \int\limits_{\Delta A_j} \mathbf{n} \cdot \nabla T(\mathbf{x}, t) \, dA$$

$$\cong \frac{\lambda}{\Delta V_i} \sum_j (\mathbf{n} \cdot \nabla T(\mathbf{x}, t)) \Delta A_j = \lambda \sum_j (\mathbf{n} \cdot \nabla T(\mathbf{x}, t)) \Phi_{i,j}$$

is defined. Here A_i is the total surface limiting the control volume Ω_i, while ΔA_j is the selected part of surface A_i, $\Phi_{i,j} = \Delta A_j / \Delta V_i$ are called the shape functions (see [37]) To obtain above relation the Gauss–Ostrogradsky theorem has been used. In a similar way, the notations related to the initial conditions are determined

(3.6)
$$\theta_i(0) \equiv \frac{\lambda}{\Delta V_i} \int\limits_{\Omega_i} \nabla^2 T(\mathbf{x}, 0) \, d\Omega = \frac{\lambda}{\Delta V_i} \int\limits_{\Omega_i} \nabla^2 T_0(\mathbf{x}) \, d\Omega$$

$$\cong \lambda \sum_j (\mathbf{n} \cdot \nabla T_0(\mathbf{x})) \Phi_{i,j}$$

which can be calculated once for every control volume.

Putting Eqs. (3.2)–(3.6) into Eq. (3.1), the following semi-discrete form of Eq. (2.18) is obtained

(3.7)
$$c \frac{dT_i(t)}{dt} \Delta V_i = \frac{\tau_T}{\tau_q} (\theta_i(t) \Delta V_i - s_q(t) \theta_i(0) \Delta V_i)$$

$$+ \int\limits_0^t K_q(t - u) \theta_i(u) \, du \, \Delta V_i$$

$$+ s_q(t)(c \bar{T}_{1i} \, \Delta V_i - Q_i(0) \Delta V_i) + Q_i(t) \Delta V_i$$

or

(3.8) $\quad c \dfrac{dT_i(t)}{dt} = \dfrac{\tau_T}{\tau_q} (\theta_i(t) - s_q(t) \theta_i(0)) + \Psi_i(t) + s_q(t)(c \bar{T}_{1i} - Q_i(0)) + Q_i(t)$

where

$$(3.9) \qquad \Psi_i(t) = \int\limits_0^t K_q(t-u)\theta_i(u)\,du.$$

The second stage of the CVM is the integration of Eq. (3.8) with respect to time. Thus, the homogeneous time grid is introduced:

$$(3.10) \qquad 0 = t^0 < t^1 < \ldots < t^{f-1} < t^f < \ldots < t^F = M, \quad t^f = f\Delta t$$
$$\text{for } f = 0,\ldots,F.$$

The effect of the integration of equation from t^{f-1} to t^f can be obtained introducing the approximation of time derivatives by the appropriate finite differences and for transition: $t^{f-1} \to t^f$, $f = 1,\ldots,F$, the following numerical scheme (here: the implicit scheme) is proposed

$$(3.11) \qquad c\frac{T_i(t^f) - T_i(t^{f-1})}{\Delta t} = \frac{\tau_T}{\tau_q}(\theta_i(t^f) - s_q(t^f)\theta_i(t^0)) + \Psi_i(t^f)$$
$$+ s_q(t^f)(c\bar{T}_{1i} - Q_i(t^0)) + \frac{Q_i(t^f) + Q_i(t^{f-1})}{2}$$

wherein the term containing the internal heat source is taken as the arithmetic mean of Q for times $f-1$ and f. Let us introduce the additional notations: $T_i^f \equiv T_i(t^f)$, $Q_i^f \equiv Q_i(t^f)$, $\theta_i^f \equiv \theta_i(t^f)$, $\Psi_i^f \equiv \Psi_i(t^f)$, $s_q^f \equiv s_q(t^f)$. Then, Eq. (3.11) can be written as

$$(3.12) \qquad c\frac{T_i^f - T_i^{f-1}}{\Delta t} = \frac{\tau_T}{\tau_q}(\theta_i^f - s_q^f\theta_i^0) + \Psi_i^f + s_q^f(c\bar{T}_{1\,i} - Q_i^0) + \frac{Q_i^f + Q_i^{f-1}}{2}.$$

The term Ψ_i^f can be approximated in the following way (by using the trapezoidal rule of integration)

$$(3.13) \qquad \Psi_i^f \equiv \Psi_i(t^f) = \int\limits_0^{t^f} K_q(t^f - u)\theta_i(u)\,du = \sum_{k=1}^{f}\int\limits_{t^{k-1}}^{t^k} K_q(t^f - u)\theta_i(u)\,du$$

$$\cong \sum_{k=1}^{f}\frac{\theta_i^k + \theta_i^{k-1}}{2}\int\limits_{t^{k-1}}^{t^k} K_q(t^f - u)\,du \cong \sum_{k=1}^{f}(\theta_i^k + \theta_i^{k-1})\hat{K}_q^{f,k}$$

$$= \hat{K}_q^{f,f}\theta_i^f + \sum_{k=1}^{f-1}(\hat{K}_q^{f,k} + \hat{K}_q^{f,k+1})\theta_i^k + \hat{K}_q^{f,1}\theta_i^0$$

where

$$(3.14) \qquad \hat{K}_q^{f,k} = \frac{1}{2} \int\limits_{t^{k-1}}^{t^k} K_q(t^f - u)\, du = \frac{1}{2}\left(1 - \frac{\tau_T}{\tau_q}\right)\exp\left(-\frac{t^f - u}{\tau_q}\right)\Bigg|_{t^{k-1}}^{t^k}$$

$$= h^f(g^k - g^{k-1})$$

and

$$(3.15) \qquad h^f = \exp\left(-\frac{f\Delta t}{\tau_q}\right),$$

$$(3.16) \qquad g^k = \frac{1}{2}\left(1 - \frac{\tau_T}{\tau_q}\right)\exp\left(\frac{k\Delta t}{\tau_q}\right) \quad \text{for } k = 0,\dots,f.$$

Further transformations of Ψ_i^f (Eq. (3.13)) lead to the formula

$$(3.17) \qquad \Psi_i^f = h^f(g^f - g^{f-1})\theta_i^f + h^f\left((g^1 - g^0)\theta_i^0 + \sum_{k=1}^{f-1}(g^{k+1} - g^{k-1})\theta_i^k\right)$$

$$= w\theta_i^f + h^f u_i^{f-1}$$

where

$$(3.18) \qquad w = h^f(g^f - g^{f-1}) = \frac{1}{2}\left(1 - \frac{\tau_T}{\tau_q}\right)\left(1 - \exp\left(-\frac{\Delta t}{\tau_q}\right)\right),$$

$$(3.19) \qquad u_i^{f-1} = (g^1 - g^0)\theta_i^0 + \sum_{k=1}^{f-1}(g^{k+1} - g^{k-1})\theta_i^k \quad \text{for } f > 0.$$

One can notice that the coefficient w does not depend on time level f.

To reduce the computation costs (i.e. the computational time and memory requirements) for the presented discrete scheme, the following recurrence relationship is introduced

$$(3.20) \qquad u_i^f = \begin{cases} u_i^{f-1} + (g^{f+1} - g^{f-1})\theta_i^f & \text{for } f > 0, \\ (g^1 - g^0)\theta_i^0 & \text{for } f = 0 \end{cases}$$

and now, to calculate these values for the successive time steps, the previous values of u_i^{f-1} can be used – this approach significantly reduces the computational time and memory requirements.

Putting Eq. (3.17) into (3.12) and after rearranging one obtains

$$(3.21) \qquad T_i^f - \frac{\Delta t}{c}\left(\frac{\tau_T}{\tau_q} + w\right)\theta_i^f$$

$$= T_i^{f-1} + \frac{\Delta t}{c}\left[h^f u_i^{f-1} - \frac{\tau_T}{\tau_q}s_q^f\theta_i^0 + s_q^f(c\bar{T}_{1i} - Q_i^0) + \frac{Q_i^f + Q_i^{f-1}}{2}\right].$$

Simultaneously, at the same level of time f for i-th control volume after the determination of T_i^f, the values of u_i^f (Eq. (3.20)) should be additionally determined. It is worth pointing out that this approach is favourable at the stage of numerical calculation.

Whereas, values of θ_i^f (see Eq. (3.5))

$$(3.22) \qquad \theta_i^f \cong \lambda \sum_j (\mathbf{n} \cdot \nabla T(\mathbf{x}, t^f)) \Phi_{i,j}$$

and the method of approximation of θ_i^f should be determined depending on discretization of the considered (1D, 2D or 3D) domain. The shape of control volumes can be defined in many ways, i.e. one of discretizations of the domain is the Voronoi mesh [37]. Proper determination of the temperature gradient on every boundary of the control volume depends on many aspects: i.e. number and shape of boundaries, the consideration of the neighbourhood of another control volume or the given type of boundary condition.

In the case of Eq. (2.29) in which the initial conditions: $T_0(\mathbf{x}) = T_{\text{init}} = \text{const}$ and $\mathbf{q}_0(\mathbf{x}) = 0$ are taken into account, the numerical scheme can be analogically derived and can be written in the form

$$(3.23) \quad T_i^f - \frac{\Delta t}{c}\left(\frac{\tau_T}{\tau_q} + w\right)\theta_i^f = T_i^{f-1} + \frac{\Delta t}{c}\left[h^f u_i^{f-1} - \frac{\tau_T}{\tau_q} s_q^f \theta_i^0 + \frac{Q_i^f + Q_i^{f-1}}{2}\right].$$

The initial condition (2.3) is implemented as

$$(3.24) \qquad T_i^0 \cong \frac{1}{\Delta V_i} \int\limits_{\Omega_i} T_0(\mathbf{x})\, d\Omega \quad \text{or} \quad T_i^0 = T_{\text{init}} \quad \text{if } T_0(\mathbf{x}) = T_{\text{init}} = \text{const.}$$

4. Application in modeling of the laser heating of thin metal film

4.1. 1D problem

To verify the correctness and exactness of the model and numerical algorithm presented previously, the 1D problem concerning the laser heating of metal film has been solved. The exact analytical solution of the same problem based on a different mathematical model was taken from [21]. Let us consider the 1D domain of thickness L: $\mathbf{x} = x$, $x \in [0, L]$. The internal heat source generated inside the domain, as the effects of the femtosecond laser pulse irradiation on the metal film surface is described by the function

$$(4.1) \qquad Q(x,t) = I_0 \sqrt{\frac{\beta}{\pi}} \frac{1 - R_f}{t_p \delta} \exp\left[-\frac{x}{\delta} - \beta \frac{(t - 2t_p)^2}{t_p^2}\right]$$

where I_0 is a laser intensity, R_f is a reflectivity of an irradiated surface of the metal, δ is an optical penetration depth, $\beta = 4\ln(2) \approx 2.773$ and t_p is a characteristic time of laser pulse. The energy of laser pulse is fed into the domain interior and its absorption takes place. The heat source function (4.1) can be also decomposed as

$$(4.2) \qquad Q(x,t) = I_0(1 - R_f)I_x(x)I_t(t)$$

where

$$(4.3) \qquad I_x(x) = \frac{1}{\delta}\exp\left(-\frac{x}{\delta}\right), \qquad I_t(t) = \sqrt{\frac{\beta}{\pi}}\frac{1}{t_p}\exp\left(-\beta\frac{(t - 2t_p)^2}{t_p^2}\right).$$

The initial conditions for the problem considered are given as $T(x,0) = T_{\text{init}}$, $\mathbf{q}_0(x) = 0$ and the adiabatic boundary conditions at boundaries are assumed in the form $q_b(0,t) = 0$, $q_b(L,t) = 0$ (this form of conditions results from the extremely short period of laser heating, e.g. [38, 39, 40])

Summing up, this problem can be described by the appropriate integro-differential equation supplemented by boundary-initial conditions, namely

$$(4.4) \qquad c\frac{\partial T(x,t)}{\partial t} = \lambda\frac{\tau_T}{\tau_q}\nabla^2 T(x,t) + \lambda\int_0^t K_q(t-u)\nabla^2 T(x,u)\,du + Q(x,t),$$

$$
\begin{aligned}
x = 0: & \quad -\lambda(\mathbf{n}\cdot\nabla T(x,t))|_{x=0} = 0, \\
x = L: & \quad -\lambda(\mathbf{n}\cdot\nabla T(x,t))|_{x=L} = 0, \\
t = 0: & \quad T(x,0) = T_{\text{init}}
\end{aligned}
$$

(4.5)

Numerical solution of the 1D problem

To solve the problem discussed, the numerical scheme described by formula (3.23) is used.

The domain considered $x \in [0, L]$ is divided into $N + 1$ control volumes Ω_i, $i = 0, \ldots, N$ with the central nodes $x_i = i\Delta x$, $\Delta x = L/N$. The geometrical mesh is presented in Fig. 1.
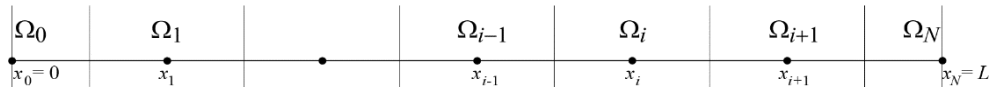

FIG. 1. Mesh of control volumes.

The areas of contact surface between two adjacent control volumes are identical and equal to ΔA, while their volumes and the shapes functions are equal to

$$
(4.6) \quad
\begin{aligned}
\Delta V_i &= \Delta x \, \Delta A \cdot
\begin{cases}
0.5 & \text{for } i = 0, N, \\
1 & \text{for } i = 1, \ldots, N-1,
\end{cases} \\[2mm]
\Phi_i &= \frac{\Delta A}{\Delta V_i} = \frac{1}{\Delta x} \cdot
\begin{cases}
2 & \text{for } i = 0, N, \\
1 & \text{for } i = 1, \ldots, N-1.
\end{cases}
\end{aligned}
$$

For the mesh presented above, one can find the values θ_i^f for $f > 0$ occurring in Eq. (3.23) (taking also into account the form of the assumed boundary conditions) and

$$
\begin{aligned}
(4.7) \quad \theta_i^f &\cong \lambda \left(
\begin{cases}
\dfrac{T_{i-1}^f - T_i^f}{\Delta x} \Phi_i & \text{if } i > 0 \\
0 & \text{if } i = 0
\end{cases}
+
\begin{cases}
\dfrac{T_{i+1}^f - T_i^f}{\Delta x} \Phi_i & \text{if } i < N \\
0 & \text{if } i = N
\end{cases}
\right) \\[3mm]
&= \frac{\lambda}{(\Delta x)^2} \cdot
\begin{cases}
2(T_1^f - T_0^f) & \text{if } i = 0 \\
T_{i-1}^f - 2T_i^f + T_{i+1}^f & \text{if } i = 1, \ldots, N-1 \\
2(T_{N-1}^f - T_N^f) & \text{if } i = N
\end{cases}
\end{aligned}
$$

whereas $\theta_i^0 = 0$ for the condition $T_i^0 = T_{\text{init}}$. Now, putting Eq. (4.7) into Eq. (3.23), the following system of $N + 1$ algebraic equation is obtained

$$
\begin{aligned}
(4.8) \quad T_i^f - \frac{\lambda \Delta t}{c(\Delta x)^2} \left(\frac{\tau_T}{\tau_q} + w \right) \cdot
&\begin{cases}
2(T_1^f - T_0^f) & \text{if } i = 0 \\
T_{i-1}^f - 2T_i^f + T_{i+1}^f & \text{if } i = 1, \ldots, N-1 \\
2(T_{N-1}^f - T_N^f) & \text{if } i = N
\end{cases} \\[3mm]
&= T_i^{f-1} + \frac{\Delta t}{c} \left(h^f u_i^{f-1} + \frac{Q_i^f + Q_i^{f-1}}{2} \right)
\end{aligned}
$$

for $i = 0, 1, \ldots, N$, $f > 0$ (for $f = 0$ see Eq. (3.24)), while the values of u_i^f (after the calculations of T_i^f) are determined (by putting Eq. (4.7) into Eq. (3.20)) and

$$
(4.9) \quad u_i^f =
$$

$$
\begin{cases}
u_i^{f-1} + (g^{f+1} - g^{f-1}) \dfrac{\lambda}{(\Delta x)^2} \cdot
\begin{cases}
2(T_1^f - T_0^f) & \text{if } i = 0 \\
T_{i-1}^f - 2T_i^f + T_{i+1}^f & \text{if } i = 1, \ldots, N-1 \\
2(T_{N-1}^f - T_N^f) & \text{if } i = N
\end{cases}
& \text{for } f > 0, \\[6mm]
0 & \text{for } f = 0.
\end{cases}
$$

The average values of the source term can be determined in an analytical way

$$(4.10) \qquad \frac{Q_i^f + Q_i^{f-1}}{2} = \frac{1}{\Delta V_i} \int\limits_{\Omega_i} \frac{Q(x, t^f) + Q(x, t^{f-1})}{2} \, d\Omega$$

$$\cong I_0(1 - R_f)\frac{I_t(t^f) + I_t(t^{f-1})}{2} \frac{1}{\Delta V_i} \int\limits_{\Omega_i} I_x(x) \, d\Omega$$

$$\cong I_0(1 - R_f)\frac{I_t(t^f) + I_t(t^{f-1})}{2} \frac{1}{\Delta x}$$

$$\cdot \begin{cases} 2\left(1 - \exp\left(-\dfrac{0.5\Delta x}{\delta}\right)\right) & \text{for } i = 0 \\[2mm] \exp\left(-\dfrac{(i - 0.5)\Delta x}{\delta}\right) - \exp\left(-\dfrac{(i + 0.5)\Delta x}{\delta}\right) & \text{for } i = 1, \ldots, N - 1 \\[2mm] 2\left(\exp\left(-\dfrac{L - 0.5\Delta x}{\delta}\right) - \exp\left(-\dfrac{L}{\delta}\right)\right) & \text{for } i = N. \end{cases}$$

The application of analytical methods at the stage of selected parameters calculations allows one to increase the accuracy of numerical solution.

Examples of numerical computations

The 1D domains of thin metal films ($L = 100$ nm) subjected to the laser pulse acting on the surface $x = 0$ are considered. Thermophysical parameters of the metals (here assumed as the constant values) are taken from [2]

– gold (Au): $c = 2.4897 \cdot 10^6$ J/(m$^3 \cdot$K), $\lambda = 315$ W/(m$\cdot$K), $\tau_q = 8.5 \cdot 10^{-12}$, $\tau_T = 90 \cdot 10^{-12}$ s,

– chromium (Cr): $c = 3.21484 \cdot 10^6$ J/(m$^3 \cdot$ K), $\lambda = 93$ W/(m $\cdot$ K), $\tau_q = 0.136 \cdot 10^{-12}$ s, $\tau_T = 7.86 \cdot 10^{-12}$ s,

– nickel (Ni): $c = 4 \cdot 10^6$ J/(m$^3 \cdot$ K), $\lambda = 90.8$ W/(m $\cdot$ K), $\tau_q = 0.82 \cdot 10^{-12}$ s, $\tau_T = 10 \cdot 10^{-12}$ s.

The parameters of the laser pulse (determining the capacity of the internal heat source; see Eq. (4.1)) [2] are equal to $I_0 = 13.7$ J/m^2, $\delta = 15.3 \cdot 10^{-9}$ m, $R_f = 0.93$ and $t_p = 0.1 \cdot 10^{-12}$ s. The initial temperature of all materials equals $T(x, 0) = T_{\text{init}} = 300$ K, while the initial heat flux $\mathbf{q}_0(x) = 0$ W/m^2.

In Figures 2–4 the temperature histories at the central points of selected control volumes and next the temperature profiles for the different moments of time are shown. The courses of the average temperatures $T_{\text{avg}}(t)$ of the whole domain are also presented. The values of T_{avg} at the moment of time t^f are calculated using the values of nodal temperatures $T_{\text{avg}}(t)|_{t=t^f} = \sum_{i=0}^{N}(T_i^f \Delta V_i)/\sum_{i=0}^{N} \Delta V_i$. The numerical calculations are performed for $\Delta x = 10^{-10}$ m ($N = 1000$) and $\Delta t = 10^{-17}$ s.
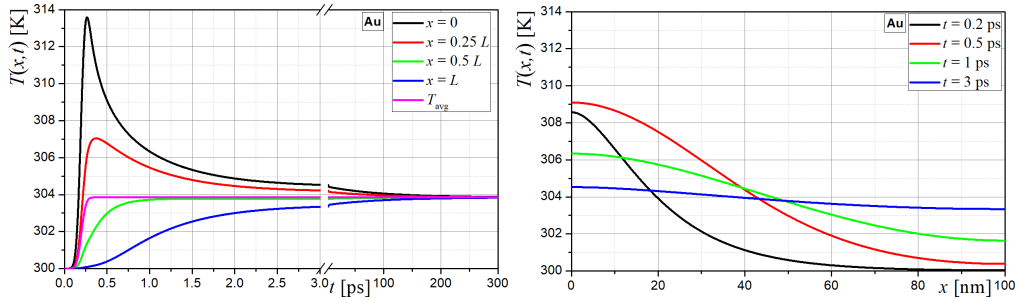
FIG. 2. Temperature history at the selected points of the domainand temperature profiles at the selected moments of time for gold (Au).

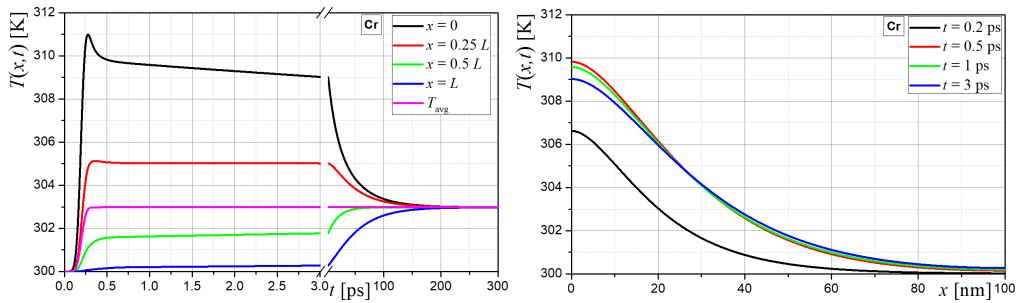FIG. 3. Temperature history at the selected points of the domainand temperature profiles at the selected moments of time for chromium (Cr).
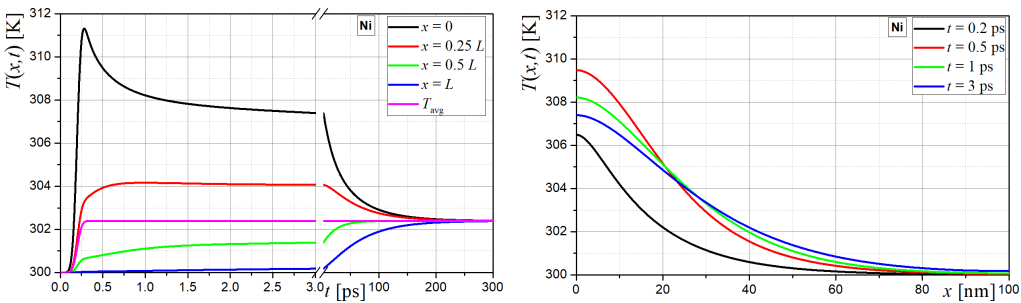

FIG. 4. Temperature history at the selected points of the domainand temperature profiles at the selected moments of time for nickel (Ni).

One can see, that the heating/cooling curves for the long simulation time (here: $300 \cdot 10^{-12}$ s) tend to the state of equilibrium (after completion of the laser pulse). The final temperature in the domain, when thermal equilibrium is reached, depends on the thermophysical parameters of metal and can be determined analytically. Thus, in this place the additional task is considered. The total energy ΔQ [J] supplied to the considered domain Ω during one laser pulse

is determined by the formula

$$(4.11) \quad \Delta Q = \int_0^\infty \int_\Omega Q(x,t)\, dx\, dt = I_0 \cdot (1 - R_f) \cdot \Delta A \cdot \int_0^L I_x(x)\, dx \cdot \int_0^\infty I_t(t)\, dt$$

$$= I_0 \cdot (1 - R_f) \cdot \Delta A \cdot \left(1 - \exp\left(-\frac{L}{\delta}\right)\right) \cdot \frac{\mathrm{erf}(2\sqrt{\beta}) + 1}{2} \text{ [J]}$$

where ΔA [m^2] is the 'virtual' side surface area of the 1D domain (plate). For above given parameters of laser: I_0, δ, R_f, t_p and the domain thickness L, the value of ΔQ is about $\Delta Q \approx 0.958 \cdot \Delta A$ [J] (and does not depend on the thermophysical parameters of the metal). The laser energy ΔQ (for $t \gg 4t_p$ and the adiabatic conditions at both boundaries of Ω) causes a rise in the average temperature T_avg in the domain by the value of $\Delta T_\mathrm{avg} = \Delta Q/(c\Delta V)$ [K], where ΔV [m^3] is the volume of the domain (in the case of the 1D domain: $\Delta V = L\Delta A$). For the assumed thermophysical parameters, the temperature T_avg after the laser action increases by values: $\Delta T_\mathrm{avg} \approx 3.85$ K (Au), $\Delta T_\mathrm{avg} \approx 2.98$ K (Cr), $\Delta T_\mathrm{avg} \approx 2.39$ K (Ni). The values of $T_\mathrm{avg} = T_\mathrm{init} + \Delta T_\mathrm{avg}$ for different metals have been used to verify the obtained numerical results. This is not exactly visible in the presented figures, but very good agreement between both values of T_avg has been obtained. Such results confirm the correctness of the numerical model and the conservation of energy in the domain.

Verification and analysis of numerical solution

The problem discussed in this paper can be also described using the classical first-order DPLE with internal heat source (4.1) supplemented by the appropriate boundary-initial conditions, this means

$$
c\left(\frac{\partial T(x,t)}{\partial t} + \tau_q \frac{\partial^2 T(x,t)}{\partial t^2}\right)
$$

$$
= \lambda\left(\frac{\partial^2 T(x,t)}{\partial x^2} + \tau_T \frac{\partial^3 T(x,t)}{\partial t\, \partial x^2}\right) + Q(x,t) + \tau_q \frac{\partial Q(x,t)}{\partial t},
$$

$$(4.12)$$

$$
\lambda\left(\frac{\partial T(x,t)}{\partial x} + \tau_T \frac{\partial^2 T(x,t)}{\partial t\, \partial x}\right)\bigg|_{x=0} = 0,
$$

$$
-\lambda\left(\frac{\partial T(x,t)}{\partial x} + \tau_T \frac{\partial^2 T(x,t)}{\partial t\, \partial x}\right)\bigg|_{x=L} = 0
$$

and

$$T(x,t)\big|_{t=0} = T_0 = \text{const},$$

$$(4.13) \quad \frac{\partial T(x,t)}{\partial t}\bigg|_{t=0} = T_1(x) = \frac{Q(x,0)}{c} = \frac{1}{c}\sqrt{\frac{\beta}{\pi}}\frac{1 - R_f}{t_p\delta}\, I_0 \exp(-4\beta)\exp\left(-\frac{x}{\delta}\right).$$

The analytical solution of the above initial-boundary value problem (under the assumption $\tau_q < \tau_T$) can be found using the appropriately modified solution presented by Ciesielski in [21]. Thus

$$(4.14) \qquad T(x,t) = U_0(t) + 2\sum_{n=1}^{\infty} \cos(\mu_n x)U_n(t) + T_0$$

where

$$(4.15) \qquad U_n(t) = \frac{1 - (-1)^n \exp(-L/\delta)}{1 + \delta^2(\mu_n)^2} \frac{(1 - R_f)I_0}{c\tau_q L} \frac{\exp(-4\beta)}{4f_n}$$

$$\times \left\{ (1 - \tau_q(d_n + f_n)) \exp((g_n^+)^2 - (d_n + f_n)t)\left[\operatorname{erfc}(g_n^+) - \operatorname{erfc}\left(g_n^+ - \sqrt{\beta}\frac{t}{t_p}\right)\right] \right.$$

$$\left. - (1 - \tau_q(d_n - f_n)) \exp((g_n^-)^2 - (d_n - f_n)t)\left[\operatorname{erfc}(g_n^-) - \operatorname{erfc}\left(g_n^- - \sqrt{\beta}\frac{t}{t_p}\right)\right] \right\}$$

$$\mu_n = \frac{n\pi}{L}, \quad d_n = \frac{1}{2\tau_q}\left(1 + \mu_n^2 \frac{\lambda}{c}\tau_T\right), \quad f_n = \sqrt{d_n^2 - \mu_n^2 \frac{\lambda}{c}\frac{1}{\tau_q}}$$

$$\text{and } g_n^{\pm} = 2\sqrt{\beta} + \frac{t_p}{2\sqrt{\beta}}(d_n \pm f_n) \text{ for } n = 0, 1, \ldots.$$

The results of this analytical solution are used at the stage of numerical results verification. The root mean square errors (E_{RMS}) between the analytic solution and numerical solutions obtained for the different values of Δt and Δx at the time level t^f are determined by the well-know formula

$$(4.16) \qquad E_{\mathrm{RMS}}(t) = \sqrt{\frac{1}{N+1}\sum_{i=0}^{N}(T_{\mathrm{analytical}}(x_i, t) - T_{\mathrm{numerical}}(x_i, t))^2}.$$

The values of $E_{\mathrm{RMS}}(t)$ for two selected time levels are listed in Table 1 (here, the thermophysical parameters of Au are taken into account). The error ratios which allow to estimate the rate of convergence for presented numerical scheme are also shown in this table. As it is well known, the error decreases with decreasing of grid size. These ratios indicate the factor by which E_{RMS} decreases when Δx and Δt decrease geometrically with quotients $1/2$ and $1/4$ (for data in the table: $m = 2$ has been assumed). For a scheme that is converging at a rate of $O((\Delta x)^2 + \Delta t)$ it is expected that the ratios are near 4 [40]. Looking at the data in Table 1, it follows that the error ratios are close to 4, hence the suggested rate of convergence is $O((\Delta x)^2 + \Delta t)$.

Table 1. Error measures E_{RMS} for numerical solutions of equation (obtained for different values of Δt and Δx) for $t = \{0.2, 0.5\}$ [ps] and the values of error ratios.

k	N $100 \cdot 2^k$	Δx [nm] $L/(100 \cdot 2^k)$	Δt [fs] $0.1/4^k$	$t = 0.2$ ps $E_{\mathrm{RMS}}(t)$	ratio	$t = 0.5$ ps $E_{\mathrm{RMS}}(t)$	ratio
0	100	1.00000	0.10000000000	0.000604478	–	0.000372228	–
1	200	0.50000	0.02500000000	0.000151251	3.9965	0.000092918	4.0060
2	400	0.25000	0.00625000000	0.000037838	3.9973	0.000023213	4.0029
3	800	0.12500	0.00156250000	0.000009463	3.9985	0.000005801	4.0014
4	1600	0.06250	0.00039062500	0.000002366	3.9992	0.000001450	4.0007
5	3200	0.03125	0.00009765625	0.000000592	3.9996	0.000000362	4.0004

In Table 2, sample numerical solutions of the considered problem for selected values of x and t are presented. The numerical results obtained for different values of Δt and Δx have been compared with analytical results and the numerical errors are also listed in Table 2. Additionally, the ratios (being factors by which numerical errors decrease when Δx is decreased by 2 and Δt by 4) are given and their values close to 4 confirm that the scheme is also converging at a rate of $O((\Delta x)^2 + \Delta t)$.

Table 2. Numerical solutions of equation (obtained for different values of Δt and Δx) for $T(0\,\mathrm{nm}, 0.2\,\mathrm{ps})$ and $T(25\,\mathrm{nm}, 0.5\,\mathrm{ps})$ with calculated numerical errors $\mathrm{Err} = T_{\mathrm{analytical}}(x,t) - T_{\mathrm{numerical}}(x,t)$ and error ratios.

k	N $100 \cdot 2^k$	Δx [nm] $L/(100 \cdot 2^k)$	Δt [fs] $0.1/4^k$	$x = 0$ nm, $t = 0.2$ ps $T(x,t)$	Err	ratio	$x = 25$ nm, $t = 0.5$ ps $T(x,t)$	Err	ratio
0	100	1.00000	0.10000000000	308.571646518	$4.700 \cdot 10^{-4}$	–	306.768765425	$3.948 \cdot 10^{-4}$	–
1	200	0.50000	0.02500000000	308.572000534	$1.160 \cdot 10^{-4}$	4.0514	306.769061563	$9.864 \cdot 10^{-5}$	4.0022
2	400	0.25000	0.00625000000	308.572087640	$2.891 \cdot 10^{-5}$	4.0128	306.769135547	$2.466 \cdot 10^{-5}$	4.0005
3	800	0.12500	0.00156250000	308.572109330	$7.222 \cdot 10^{-6}$	4.0032	306.769154040	$6.164 \cdot 10^{-6}$	4.0001
4	1600	0.06250	0.00039062500	308.572114747	$1.805 \cdot 10^{-6}$	4.0008	306.769158663	$1.541 \cdot 10^{-6}$	4.0000
5	3200	0.03125	0.00009765625	308.572116101	$4.513 \cdot 10^{-7}$	4.0001	306.769159819	$3.853 \cdot 10^{-7}$	3.9996
Analytical solutions $T_{\mathrm{analytical}}(x,t)$:			308.572116552			306.769160204		

4.2. 2D axially-symmetrical problem

The second, more practical example concerns 2D axially-symmetrical task (the solution obtained is 3D, of course). The considered domain Ω (see Fig. 5) is limited by the planes $z = 0$, $z = Z$ and surface $r = R$, the point of domain Ω has coordinates $\mathbf{x} = (r, z)$, $r \in [0, R]$, $z \in [0, Z]$.

The heating process of metal occurring in this domain is realized due to the femtosecond laser pulse irradiation (the Gaussian laser beam) on the upper surface limiting the system. The internal heat source $Q(r, z, t)$ generated inside
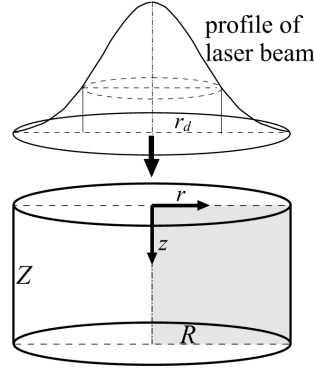
FIG. 5. Cylindrical micro-domain.

the domain is related with the absorption of laser beam and here, it is assumed as

$$(4.17) \qquad Q(r,z,t) = \sqrt{\frac{\beta}{\pi}} \frac{1-R_f}{t_p \delta} I_0 \exp\left(-\frac{r^2}{r_d^2} - \frac{z}{\delta} - \beta\frac{(t-2t_p)^2}{t_p^2}\right)$$

$$= I_0(1-R_f)I_{rz}(r,z)I_t(t)$$

where

$$(4.18) \qquad I_{rz}(r,z) = \frac{1}{\delta}\exp\left(-\frac{z}{\delta}\right)\exp\left(-\frac{r^2}{r_d^2}\right),$$

$$I_t(t) = \sqrt{\frac{\beta}{\pi}}\frac{1}{t_p}\exp\left(-\beta\frac{(t-2t_p)^2}{t_p^2}\right)$$

and r_d is a characteristic radius of Gaussian laser beam. The remaining notations are the same as in Eq. (4.1). Assuming large enough dimensions Z and R of the considered domain (relative to the parameters of the Gaussian laser beam), the adiabatic boundary conditions on the appropriate boundaries Γ can be accepted: $(r,z) \in \Gamma : q_b(r,z,t) = 0$. Also, the initial conditions for this considered task are given in the forms $T(r,z,0) = T_{\text{init}}$ and $\mathbf{q}_0(r,z) = 0$.

Taking into account the above considerations, the heating process of metal occurring in the axially-symmetrical domain can be described by the following integro-differential equation supplemented by boundary-initial conditions

$$c\frac{\partial T(r,z,t)}{\partial t} = \lambda\frac{\tau_T}{\tau_q}\nabla^2 T(r,z,t) + \lambda\int_0^t K_q(t-u)\nabla^2 T(r,z,u)\,du + Q(r,z,t),$$

$$(4.19)$$
$$r \in \{0,R\}: \quad -\lambda(\mathbf{n}{\cdot}\nabla T(r,z,t))|_{r=0} = -\lambda(\mathbf{n}{\cdot}\nabla T(r,z,t))|_{r=R} = 0,$$
$$z \in \{0,Z\}: \quad -\lambda(\mathbf{n}{\cdot}\nabla T(r,z,t))|_{z=0} = -\lambda(\mathbf{n}{\cdot}\nabla T(r,z,t))|_{z=Z} = 0,$$
$$t = 0: \quad T(r,z,0) = T_{\text{init}}.$$

Examples of numerical computations

The cylindrical domain of gold (Au) with dimensions $Z = 100 \cdot 10^{-9}$ m, $R = 100 \cdot 10^{-9}$ m is considered. Thermophysical parameters of gold are earlier given in the description of the 1D simulation. The parameters of the laser pulse are identical as before, and additionally $r_d = 50 \cdot 10^{-9}$ m. The initial temperature is equal to: $T(r, z, 0) = T_{\text{init}} = 300$ K.

The considered domain of cylinder is divided into small regular control volumes. The shape of control volumes corresponds to the rings of a rectangular cross-section. Here, the number of control volumes is equal to $(N_r + 1) \cdot (N_z + 1)$, while the distances between two central nodes in a rectangular cross-section of neighbouring control volumes are equal to $\Delta r = R/N_r$ and $\Delta z = Z/N_z$, respectively. Details about the construction of geometrical mesh for the axially-symmetrical domain one can find in our previous works [29, 30].
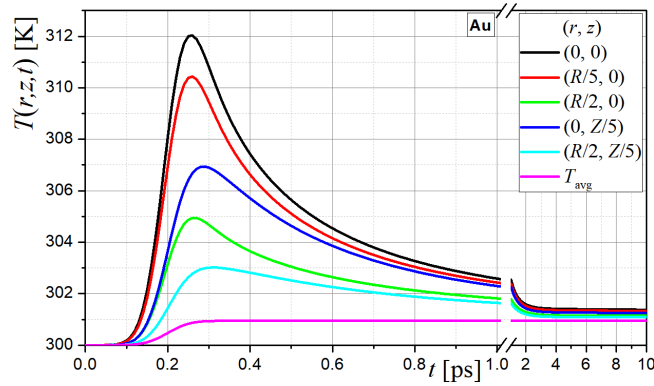

FIG. 6. Heating curves at the selected control volumes containing points (r, z) and average temperature of whole domain.

In Fig. 6, the temperature histories at the five selected control volumes of the domain are shown. Also, the course of the average temperature T_{avg} of the whole cylindrical domain is presented in this figure. The calculations are performed for the following mesh parameters: $\Delta z = 10^{-9}$ m, $\Delta r = 10^{-9}$ m, $\Delta t = 10^{-16}$ s.

The courses of isotherms for the selected moments of time: $t = \{0.2, 0.3, 0.4, 0.5, 1, 10 \text{ ps}\}$ are presented in Fig. 7.

The analytical solution of the 2D discussed problem is so far unknown. Hence, the verification of numerical results with analytical one is not possible.

Thus, the comparison of numerical results obtained for the different sizes of meshes has been studied. The adequate numerical simulations for different mesh steps: Δz, Δr and different time step Δt (other parameters used in the simulation remained unchanged) have been done. The differences in the numerical solutions are small and hard to visual on the graphs. So, the numerical results at the
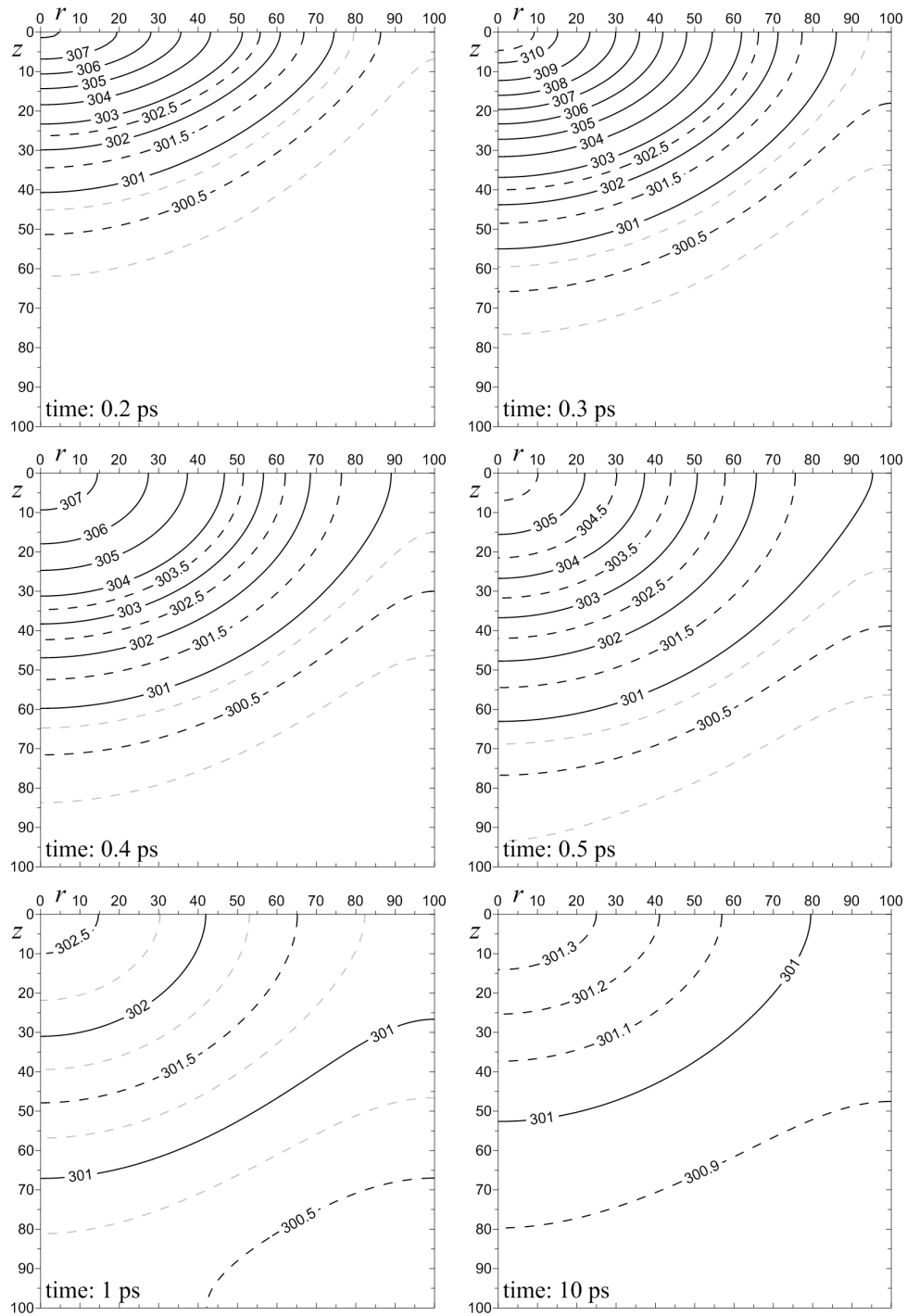
FIG. 7. Courses of isotherms in cross-section of domain for different times.

selected control volumes for time $t = 0.3$ ps and the different sizes of meshes are collected in Table 3.

Table 3. Numerical results (temperature) for different sizes of meshes.

$\Delta r = \Delta z$ [m]	Δt [s]	Average temperature [K] at time $t = 0.3$ ps in the selected control volumes containing points $P(r,z)$				
		$P_A(0,0)$	$P_B(R/5,0)$	$P_C(R/2,0)$	$P_D(0,Z/5)$	$P_E\ (R/2,Z/5)$
$2 \cdot 10^{-9}$ $(N_r = N_z = 50)$	10^{-15}	310.8002866	309.4424423	304.6728847	306.8860957	303.0066583
	10^{-16}	310.8038207	309.4455771	304.6742349	306.8941018	303.0091937
	10^{-17}	310.8041729	309.4458895	304.6743693	306.8949032	303.0094472
10^{-9} $(N_r = N_z = 100)$	10^{-15}	310.7990307	309.4413777	304.6723077	306.8891240	303.0079648
	10^{-16}	310.8025662	309.4445143	304.6736597	306.8971445	303.0105068
	10^{-17}	310.8029185	309.4448268	304.6737942	306.8979473	303.0107609
$5 \cdot 10^{-10}$ $(N_r = N_z = 200)$	10^{-15}	310.7987246	309.4411186	304.6721669	306.8898792	303.0082908
	10^{-16}	310.8022603	309.4442555	304.6735193	306.8979032	303.0108344
	10^{-17}	310.8026126	309.4445681	304.6736538	306.8987064	303.0110887

In this task, the total energy applied to the considered axially-symmetrical domain during one laser pulse is equal to

$$(4.20) \qquad \Delta Q = \int_0^\infty \int_\Omega Q(\mathbf{x}, t)\, d\mathbf{x}\, dt$$

$$= I_0 \cdot (1 - R_f) \cdot \int_0^{2\pi} \int_0^Z \int_0^R I_{rz}(r,z) \cdot r\, dr\, dz\, d\varphi \cdot \int_0^\infty I_t(t)\, dt$$

$$= I_0 \cdot (1 - R_f) \cdot \pi r_d^2 \left(1 - \exp\left(-\frac{R^2}{r_d^2} \right) \right) \left(1 - \exp\left(-\frac{Z}{\delta} \right) \right) \frac{\mathrm{erf}(2\sqrt{\beta}) + 1}{2} \quad \text{[J]}.$$

For the above assumed dimensions of cylinder and parameters of laser pulse, one can determine $\Delta Q \approx 7.38 \cdot 10^{-15}$ J in the volume of cylinder $\Delta V = \pi R^2 Z \approx 3.14 \cdot 10^{-21}$ m^3. On this basis the average temperature in the domain increases by $\Delta T_{\mathrm{avg}} \approx 0.944$ K after one laser pulse (for $t \gg 4t_p$). This value has been used to verify the correctness of the obtained numerical results. It should be pointed out that the average temperatures in the domain calculated on the base of numerical values obtained for the different sizes of meshes (Δz, Δr and Δt) for $t = 1$ ps differ from the value ΔT_{avg} by less than 10^{-9} K (for the set of all sizes of meshes given in Table 3). This test confirms the correctness of the calculations and the conservation of energy in the domain considered.

5. Conclusions

In this work, the new version of the dual-phase lag equation is proposed. In a place of the hyperbolic equation the parabolic one is obtained. In other words, in contrast to the classical form of the first-order DPLE which contains the first and the second derivative of temperature with respect to time, the new form of equation contains only the first order derivative. In turn, on the right hand side of the modified DPLE, the definite integral appears. From the computational point of view, this integral calculation is quite simple and relies on the addition of successive its increment to the value determined in the previous time steps level (so-called a cumulative sum/integral). Thus, one does not need to store in the computer memory the whole history of nodal temperatures. It should be pointed out that modification of DPLE is connected with the appropriate changes to the boundary-initial conditions The new form of DPLE, according to the authors, provides some improvements to the classical dual-phase lag equation. This is particularly evident at the stage of derivation of the numerical schemes.

The integro-differential DPLE has been solved numerically using the Control Volume Method. Both the 1D task and also the axially-symmetrical problems have been considered. The particular stages of numerical scheme construction have been described in details. The proposed implicit scheme is unconditionally stable, but the value of time step should be properly specified, especially in order to assure a good approximation of the local and temporary internal heat source function.

Some values of coefficients in the numerical scheme can be determined analytically and this approach ensures a more accurate approximation of the numerical results. The proposed general numerical scheme can be used to solve 1D, 2D and 3D tasks, it depends only on the shape of control volumes used at the stage of discretization.

In this paper, the numerical scheme for 1D domain is described in details. The results of numerical computations have been compared with other results corresponding to the analytical solution presented in [21]. Very detailed conclusions resulting from these comparisons are formulated in Section 4.

Details on heating/cooling curves and temporary temperature fields obtained for different materials are not discussed here because they do not deviate qualitatively from the solutions presented in other papers.

Considering the real values of the metals thermophysical parameters and changing over a wide range the mesh densities (Δt and Δx) one can conclude that presented implicit numerical scheme is always unconditionally stable. From the practical point of view the proper choice of Δt depends on the task considered. For example, when the problem of the femtosecond laser heating of metal film is

considered then the total laser pulse duration should be divided into 100–1000 time steps in order to assure a good approximation of the heat source function. It also seems reasonable the selection of the time grid assuring the relations $\Delta t \ll \tau_q$ and $\Delta t \ll \tau_T$.

It should be noted that using the dual-phase lag equation for numerical modeling of thermal processes, the physical anomalies can take place. The problem of mutual relations between delay times ensuring obtaining the correct solution is emphasized above all [42–44]. When $\tau_T > \tau_q$ the DPL model might violate the second law of thermodynamics and this case is defined as over-diffusion [22, 42]. Such a phenomenon can be explained by the non-equilibrium theory of entropy production [45]. On the other hand, the thermalization time τ_T and the relaxation time τ_q are the individual parameters depending on the type of materials and one can find the situation when $\tau_T > \tau_q$. Nevertheless, the results obtained as a part of the authors' research and the results presented in many other papers concerning the laser heating of thin metal layers, show that in this case the solutions obtained are, as a rule, correct both from qualitative and quantitative points of view. In turn, in [46] the discussion concerning the incorrect ways of delay times experimental determination can be found.

In the future, the authors plan to extend the presented approach on the case of the non-homogeneous domains, i.e. the heating of multi-layered thin metal films subjected to the laser beam. Here, the continuity condition on the contact surface between sub-domains should be appropriately formulated and implemented for the model described by the system of the integro-differential DPLE. The possibility of melting and resolidification should be also taken into account. We also intend to adapt the approach proposed to the case of the second-order DPLE.

Highlights

A new form of the first order dual phase lag equation is proposed.

The numerical algorithm of the problem solution based on the Control Volume Method is presented.

The problem of heating/cooling processes in domain of thin metal film subjected to a laser pulse are considered.

The results obtained were compared in detail with the analytical solution of a similar task.

Competing interests

The authors declare that they have no competing interests.

References

1. Z.M. Zhang, *Nano/Microscale Heat Transfer*, McGraw-Hill, New York, 2007.

2. D.Y. Tzou, *Macro- to Microscale Heat Transfer: the Lagging Behavior*, 2nd Ed., Wiley, New York, 2014.

3. Y. Zhang, D.Y. Tzou, J.K. Chen, *Micro- and nanoscale heat transfer in femtosecond laser processing of metals*, [in:] P.H. Barret, M. Palmerm [eds.], *High-power and Femtosecond Lasers: Properties, Materials and Applications.* pp. 159–206 (Chapter 5), Nova Science Publishers, Inc., Hauppauge, 2009.

4. A.N. Smith, P.M. Norris, *Microscale heat transfer*, [in:] A. Bejan, A.D. Kraus [eds.], *Heat Transfer Handbook*, Chap. 18, pp. 1309–1357, John Willey & Sons, Hoboken, New York, USA, 2003.

5. E. Majchrzak, B. Mochnacki, A.L. Greer, J.S. Suchy, *Numerical modeling of short-pulse laser interactions with multi-layered thin metal films*, Computer Modeling in Engineering & Sciences, **41**, 2, 131–146, 2009.

6. C.P. Grigoropoulos, A.C. Chimmalgi, D.J. Hwang, *Nano-structuring using pulsed laser irradiation*, [in:] C. Phipps [ed.], *Laser Ablation and its Applications*, **129**, Springer Series in Optical Sciences, 473–504, 2007.

7. C. Cattaneo, *A form of heat conduction equation which eliminates the paradox of instantaneous propagation*, Comptes Rendus, **247**, 431–433, 1958.

8. K.K. Tamma, X. Zhou, *Macroscale and microscale thermal transport and thermomechanical interactions: some noteworthy perspectives*, Journal of Thermal Stresses, **21**, 3-4, 405–449, 1998.

9. D.Y. Tzou, *A unified field approach for heat conduction from macro- to micro-scales*, Journal of Heat Transfer, **117**, 1, 8–16, 1995.

10. R.A. Escobar, S.S. Ghai, M.S. Jhon, C.H. Amon, *Multi-length and time scale thermal transport using the lattice Boltzmann method with application to electronics cooling*, International Journal of Heat and Mass Transfer, **49**, 1-2, 97–107, 2006.

11. J. Cabrera, M.A. Castro, F. Rodríquez, J.A. Martín, *Difference schemes for numerical solutions of lagging models of heat conduction*, Mathematical and Computer Modelling, **57**, 7-8, 1625–1632, 2013.

12. E. Majchrzak, B. Mochnacki, *Implicit scheme of the finite difference method for the second-order dual phase lag equation*, Journal of Theoretical and Applied Mechanics, **56**, 2, 393–402, 2018.

13. S. Chiriţă, M. Ciarletta, V. Tibullo, *On the thermomechanical consistency of the time differential dual-phase-lag models of heat conduction*, International Journal of Heat and Mass Transfer, **114**, 277–285, 2017.

14. E. Majchrzak, B. Mochnacki, *First and second order dual phase lag equation. Numerical solution using the explicit and implicit schemes of the finite difference method*, MATEC Web of Conferences ICCHMT, **240**, 05018, 2018.

15. W. Dai, R. Nassar, *A compact finite difference scheme for solving a three-dimensional heat transport equation in a thin film*, Numerical Methods for Partial Differential Equations, **16**, 5, 441–458, 2000.

16. S. CHIRIŢĂ, *High-order effects of thermal lagging in deformable conductors*, International Journal of Heat and Mass Transfer, **127**, 965–974, 2018.

17. D. DENG, Y. JIANG, D.Y. LIANG, *High-order finite difference methods for a second order dual-phase-lagging models of microscale heat transfer*, Applied Mathematics and Computation, **309**, 31–48, 2017.

18. R. QUINTANILLA, R. RACKE, *A note on stability in dual-phase lag heat conduction*, International Journal of Heat and Mass Transfer, **49**, 7-8, 1209–1213, 2006.

19. H. ASKARIZADEH, E. BANIASADI, H. AHMADIKIA, *Equilibrium and non-equilibrium thermodynamic analysis of high-order dual-phase-lag heat conduction*, International Journal of Heat and Mass Transfer, **104**, 301–309, 2017.

20. M. FABRIZIO, B. LAZZARI, *Stability and second law of thermodynamics in dual-phase-lag heat conduction*, International Journal of Heat and Mass Transfer, **74**, 484–489, 2014.

21. M. CIESIELSKI, *Analytical solution of the dual phase lag equation describing the laser heating of thin metal film*, Journal of Applied Mathematics and Computational Mechanics, **16**, 1, 33–40, 2017.

22. D.W. TANG, N. ARAKI, *Wavy, wavelike, diffusive thermal responses of finite rigid slabs to high-speed heating of laser-pulses*, International Journal of Heat and Mass Transfer, **42**, 5, 855–860, 1999.

23. K. RAMADAN, *Semi-analytical solutions for the dual phase lag heat conduction in multilayered media*, International Journal of Thermal Sciences, **48**, 1, 14–25, 2009.

24. S. KUMAR, A. SRIVASTAVA, *Finite integral transform-based analytical solutions of dual phase lag bio-heat transfer equation*, Applied Mathematical Modelling, **52**, 378–403, 2017.

25. K.C. LIU, J.C. WANG, *Analysis of thermal damage to laser irradiated tissue based on the dual-phase-lag model*, International Journal of Heat and Mass Transfer, **70**, 621–628, 2014.

26. V. MOHAMMADI-FAKHAR, S.H. MOMENI-MASULEH, *An approximate analytic solution of the heat conduction equation at nanoscale*, Physics Letters A, **374**, 4, 595–604, 2010.

27. M.A. CASTRO, F. RODRÍGUEZ, J. ESCOLANO, J.A. MARTÍN, *Exact and analytic-numerical solutions of lagging models of heat transfer in a semi-infinite medium*, Abstract and Applied Analysis, ID 397053, p. 6, 2013.

28. H. WANG, W. DAI, R. MELNIK, *A finite difference method for studying thermal deformation in a double-layered thin film exposed to ultrashort pulsed lasers*, International Journal of Thermal Sciences, **45**, 12, 1179–1196, 2006.

29. M. CIESIELSKI, *Application of the Alternating Direction Implicit Method for numerical solution of the dual-phase lag equation*, Journal of Theoretical and Applied Mechanics, **55**, 3, 839–852, 2017.

30. B. MOCHNACKI, M. CIESIELSKI, *Dual phase lag model of melting process in domain of metal film subjected to an external heat flux*, Archives of Foundry Engineering, **16**, 4, 85–90, 2016.

31. R. EYMARD, T. GALLOUËT, R. HERBIN, *Finite volume methods*, [in:] P.G. Ciarlet, J.L. Lions [eds.], *Techniques of Scientific Computing,* Part III, Handbook of Numerical Analysis, VII, 713–1020, North-Holland, Amsterdam, 2000.

32. H.K. Versteeg, W. Malalasekera, *An Introduction To Computational Fluid Dynamics: The Finite Volume Method*, 2nd ed., Pearson Education, Harlow, 2007.

33. E. Majchrzak, *General boundary element method for the dual-phase lag equations describing the heating of two-layered thin metal films*, [in:] A. Öchsner, H. Altenbach [eds.], Engineering Design Applications II, Advanced Structured Materials, **113**, 263–278, 2019.

34. N. Bazarra, M.I.M. Copetti, J.R. Fernandez, R. Quintanilla, *Numerical analysis of some dual-phase-lag models*, Computers & Mathematics with Applications, **77**, 2, 407–426, 2019.

35. A.D. Polyanin, V.F. Zaitsev, *Handbook of Ordinary Differential Equations: Exact Solutions, Methods, and Problems*, 3rd ed., Chapman and Hall/CRC, UK, 2018.

36. D.D. Joseph, L. Preziosi, *Heat waves*, Reviews of Modern Physics, **61**, 1, 41–73, 1989.

37. M. Ciesielski, B. Mochnacki, *Hyperbolic model of thermal interactions in a system biological tissue-protective clothing subjected to an external heat source*, Numerical Heat Transfer, Part A: Applications, **74**, 11, 1685–1700, 2018.

38. T.Q. Qiu, C.L. Tien, *Heat transfer mechanisms during short-pulse laser heating of metals*, ASME Journal of Heat Transfer, **115**, 4, 835–841, 1993.

39. T.Q. Qiu, T. Juhasz, C. Suarez. W.E. Bron, C.I. Tien, *Femtosecond laser heating of multi-layer metals – II Experiments*, International Journal of Heat and Mass Transfer, **37**, 17, 2799–2808, 1994.

40. J.K. Chen, J.E. Beraun, *Numerical study of ultrashort laser pulse interactions with metal films*, Numerical Heat Transfer, Part A: Applications, **40,** 1, 1–20, 2001.

41. S.A. Richards, *Completed Richardson extrapolation in space and time*, Communications in Numerical Methods in Engineering, **13**, 7, 573–582, 1997.

42. B. Shen, P. Zhang, *Notable physical anomalies manifested in non-Fourier heat conduction under the dual-phase-lag model*, International Journal of Heat and Mass Transfer, **51**, 7-8, 1713–1727, 2008.

43. M. Wang, N. Yang, Z.-Y. Guo, *Non-Fourier heat conductions in nanomaterials*, Journal of Applied Physics, **110**, 064310, 7 pp, 2011.

44. S.A. Rukolaine, *Unphysical effects of the dual-phase-lag model of heat conduction*, International Journal of Heat and Mass Transfer, **78**, 58–63, 2014.

45. M.A. Al-Nimr, M. Naji, V.S. Arbaci, *Nonequilibrium entropy production under the effect of the dual-phase-lag heat conduction model*, ASME Journal of Heat Transfer, **122**, 2, 217–223, 2000.

46. D. Maillet, *A review of the models using the Cattaneo and Vernotte hyperbolic heat equation and their experimental validation*, International Journal of Thermal Sciences, **139**, 424–432, 2019.